

Chaotic behavior of the closed loop thermosyphon model with memory effects

Justine Yasappan, Ángela Jiménez-Casas¹, and Mario Castro²

- ¹ Grupo de Dinámica No Lineal (DNL), Escuela Técnica Superior de Ingeniería (ICAI), Universidad Pontificia Comillas, Madrid E-28015, Spain
(E-mails: justemasj@gmail.com, ajimenez@dmc.icaei.upcomillas.es)
- ² ICAI, Grupo Interdisciplinar de Sistemas Complejos (GISC) and DNL, Universidad Pontificia Comillas, Madrid E-28015, Spain
(E-mail: marioc@upcomillas.es)

Abstract. This paper presents the motion of a viscoelastic fluid in the interior of a closed loop thermosyphon. A viscoelastic fluid described by the Maxwell constitutive equation is considered for the study. This kind of fluids present elastic-like behaviors and memory effects. Numerical experiments are performed in order to describe the chaotic behavior of the solution for different ranges of the relevant parameters by using the inertial manifold for this system proved in [1]. This work comes to verify the complex nature of the behavior of viscoelastic fluids extending the result in [2] when we consider a given heat flux instead of Newton's linear cooling law.

Keywords: Thermosyphon, Viscoelastic fluid, Asymptotic behavior, Numerical analysis.

1 Introduction

Chaos in fluids subject to temperature gradients has been the subject of intense work for its applications in the field of engineering or atmospheric sciences. A thermosyphon is a device composed of a closed loop *pipe* containing a fluid whose motion is driven by the effect of several actions such as gravity and natural convection [3–5]. The flow inside the loop is driven by an energetic balance between thermal energy and mechanical energy. The interest on this system comes both from engineering and as a *toy* model of natural convection (for instance, to understand the origin of chaos in atmospheric systems). The theoretical results of the behavior of viscoelastic fluids of this model has been proved in [1] but in this work we explore it numerically.

As viscoelasticity is, in general, strongly dependent on the material composition and working regime, here we will approach this problem by studying the most essential feature of viscoelastic fluids: memory effects. To this aim we restrict ourselves to the study of the so-called Maxwell model [6]. In this



model, both Newton's law of viscosity and Hooke's law of elasticity are generalized and complemented through an evolution equation for the stress tensor, σ . The stress tensor comes into play in the equation for the conservation of momentum:

$$\rho \left(\frac{\partial \mathbf{v}}{\partial t} + \mathbf{v} \cdot \nabla \mathbf{v} \right) = -\nabla p + \nabla \cdot \sigma \quad (1)$$

For a Maxwellian fluid, the stress tensor takes the form:

$$\frac{\mu}{E} \frac{\partial \sigma}{\partial t} + \sigma = \mu \dot{\gamma} \quad (2)$$

where μ is the fluid viscosity, E the Young's modulus and $\dot{\gamma}$ the shear strain rate (or rate at which the fluid deforms). Under stationary flow, the equation (2) reduces to Newton's law, and consequently, the equation (1) reduces to the celebrated Navier-Stokes equation. On the contrary, for short times, when *impulsive* behavior from rest can be expected, equation (2) reduces to Hooke's law of elasticity.

The derivation of the thermosyphon equations of motion is similar to that in [3–5]. The simplest way to incorporate equation (2) into equation (1) is by differentiating equation (1) with respect to time and replacing the resulting time derivative of σ with equation (2). This way to incorporate the constitutive equation allows to reduce the number of unknowns (we remove σ from the system of equations) at the cost of increasing the order of the time derivatives to second order. The resulting second order equation is then averaged along the loop section (as in Ref.[3]). Finally, after adimensionalizing the variables (to reduce the number of free parameters) we arrive at the main system of equations

$$\begin{cases} \varepsilon \frac{d^2 v}{dt^2} + \frac{dv}{dt} + G(v)v = \oint T f, & v(0) = v_0, \frac{dv}{dt}(0) = w_0 \\ \frac{\partial T}{\partial t} + v \frac{\partial T}{\partial x} = h(x) + \nu \frac{\partial^2 T}{\partial x^2}, & T(0, x) = T_0(x) \end{cases} \quad (3)$$

where $v(t)$ is the velocity, $T(t, x)$ is the distribution of the temperature of the viscoelastic fluid in the loop, ν is the temperature diffusion coefficient, $G(v)$ is the friction law at the inner wall of the loop, the function f is the geometry of the loop and the distribution of gravitational forces, $h(x)$ is the general heat flux and ε is the viscoelastic parameter, which is the dimensionless version of the viscoelastic time, $t_V = \mu/E$. Roughly speaking, it gives the time scale in which the transition from elastic to fluid-like occurs in the fluid. We consider G and h are given continuous functions, such that $G(v) \geq G_0 > 0$, and $h(v) \geq h_0 > 0$, for G_0 and h_0 positive constants. Finally, for physical consistency, it is important to note that all functions considered must be 1-periodic with respect to the spatial variable.

2 Inertial manifold: Finite dimensional asymptotic behavior

In this section we summarize the main results related to the finite dimensional asymptotic behavior of the system of equations (3) as proved in [1]. The ex-

istence and uniqueness of the solutions of (3) was proved in [1] following the techniques used in [2]. The main idea in [2] is that we rewrite our main equations (3) in terms of the Fourier expansions of each function and observing the dynamics of each Fourier mode, where $h, f \in \dot{L}_{per}^2(0, 1)$ are given by the following Fourier expansions:

$$h(x) = \sum_{k \in D} b_k e^{2\pi k i x}, f(x) = \sum_{k \in D} c_k e^{2\pi k i x}$$

with $D = D - \{0\}$ while $T_0 \in \dot{H}_{per}^1(0, 1)$ is given by

$$T_0(x) = \sum_{k \in D} a_{k0} e^{2\pi k i x}$$

and $T(t, x) \in \dot{H}_{per}^1(0, 1)$ is given by

$$T(t, x) = \sum_{k \in D} a_k(t) e^{2\pi k i x}$$

where

$$\dot{L}_{per}^2(0, 1) = \{u \in L_{loc}^2(\mathbb{R}), u(x+1) = u(x) a.e., \oint u = 0\}, \dot{H}_{per}^m(0, 1) = H_{loc}^m(\mathbb{R}) \cap \dot{L}_{per}^2(0, 1). \quad (4)$$

The coefficients $a_k(t)$ verify the equation:

$$\dot{a}_k(t) + (2\pi k \nu i + 4\nu\pi^2 k^2) a_k(t) = b_k, \quad a_k(0) = a_{k0}, \quad k \in D.$$

Here, we assume that $h \in \dot{H}_{per}^m$ with

$$h(x) = \sum_{k \in K} b_k e^{2\pi k i x}$$

where $b_k \neq 0$, for every $k \in K \subset D$ with $0 \notin K$, since $\oint h = 0$. We denote by V_m the closure of the subspace of \dot{H}_{per}^m generated by $\{e^{2\pi k i x}, k \in K\}$. If $b_k = 0$ then the k th mode for the temperature is dumped out exponentially and therefore the space V_m attracts the dynamics for the temperature. Moreover if K is a finite set, the dimension of \mathcal{M} is $|K| + 2$, where $|K|$ is the number of elements in K .

Under the above hypotheses we assume that

$$f(x) = \sum_{k \in J} c_k e^{2\pi k i x}$$

with $c_k \neq 0$ for every $k \in J \subset D$. Then on the inertial manifold we have:

$$\oint (T \cdot f) = \sum_{k \in K} a_k(t) \bar{c}_k = \sum_{k \in K \cap J} a_k(t) \bar{c}_k.$$

Therefore the evolution of velocity v , and acceleration w depends only on the coefficients of T which belong to the set $K \cap J$. From [1], using similar techniques as in [7,8] we will reduce the asymptotic behavior of the initial

system (3) to the dynamics of the reduced explicit nonlinear system of ODE's (5) where we consider the relevant modes of temperature $a_k, k \in K \cap J$.

$$\begin{cases} \frac{dw}{dt} + \frac{1}{\varepsilon}w + \frac{1}{\varepsilon}G(v)v &= \frac{1}{\varepsilon} \sum_{k \in K \cap J} a_k(t)\bar{c}_k w(0) = w_0 \\ \frac{dv}{dt} &= w, & v(0) = v_0 \\ \dot{a}_k(t) + (2\pi kvi + 4\nu\pi^2k^2)a_k(t) &= b_k, & a_k(0) = a_{k0}, \quad k \in K \cap J. \end{cases} \quad (5)$$

Note that the set $K \cap J$ can be much smaller than the set K and therefore the reduced subsystem may possess far fewer degrees of freedom than the system on the inertial manifold. Also note that it may be the case that K and J are infinite sets, but their intersection is finite. For instance, for a circular circuit we have $f(x) \sim a \sin(x) + b \cos(x)$, i.e., $J = \{\pm 1\}$ and then $K \cap J$ is either $\{\pm 1\}$ or the empty set.

3 Numerical experiments

3.1 Preliminary mathematical approximation

In this section, we integrate the system of ODEs (5), where we consider only the coefficients of temperature $a_k(t)$ with $k \in K \cap J$ (relevant modes). Thus,

$$\begin{cases} \frac{dw}{dt} + \frac{w}{\varepsilon} + \frac{G(v)v(t)}{\varepsilon} = \frac{2}{\varepsilon} \text{Real} \left(\sum_{k \in K \cap J} a_k(t)\bar{c}_k \right) & w(0) = w_0 \\ \frac{dv}{dt} = w, & v(0) = v_0 \\ \dot{a}_k(t) + a_k(t)(2\pi kiv + \nu 4\pi^2k^2) = b_k, & a_k(0) = a_{k0}. \end{cases}$$

We impose that all the physical observable as real functions, then $a_{-k} = \bar{a}_k$, $b_{-k} = \bar{b}_k$ and $c_{-k} = \bar{c}_k$. In particular, we consider a thermosyphon with a circular geometry, so $J = \{\pm 1\}$ and $K \cap J = \{\pm 1\}$. Consequently, we can take $k = 1$ and omit the equation for $k = -1$ (is conjugated of the equation for $k = 1$). Also in order to reduce the number of free parameters we make the following change of variables $a_1c_{-1} \rightarrow a_1$.

$$\begin{cases} \frac{dw}{dt} = \frac{2a_1}{\varepsilon} - \frac{w}{\varepsilon} - \frac{G(v)v(t)}{\varepsilon}, & w(0) = w_0 \\ \frac{dv}{dt} = w, & v(0) = v_0 \\ \dot{a}_1(t) + a_1(t)(2\pi iv + \nu 4\pi^2) = b_1, & a_1(0) = a_{10}. \end{cases}$$

We denote the real and imaginary parts of the $a_1(t)$ (the Fourier mode of the temperature) in the following way:

$$a_1(t) = a^1(t) + ia^2(t), \quad (6)$$

$$b_1 = A + iB \quad (7)$$

with $A \in \mathbb{R}, B \in \mathbb{R}$. Thus we obtain the corresponding nonlinear system of equations where we need to make explicit choice of the constitutive laws for both the fluid-mechanical and thermal properties for this model:

$$\begin{cases} \frac{dw}{dt} = \frac{2a^1}{\varepsilon} - \frac{w}{\varepsilon} - \frac{G(v)v(t)}{\varepsilon}, & w(0) = 0 \\ \dot{v} = w, & v(0) = 0 \\ \dot{a}^1 = A - \nu 4\pi^2a^1 + v2\pi a^2, & a^1(0) = 1 \\ \dot{a}^2 = B - \nu 4\pi^2a^2 - v2\pi a^1 & a^2(0) = 1. \end{cases} \quad (8)$$

Hereafter, we present the numerical experiments of equations (5) that are carried out for the resolution of the nonlinear system of ODEs using the fourth-order explicit Runge-Kutta method. The summary of our results is presented in the figures of section 3.2. In particular, we present the plots for velocity, acceleration and (the fourier transform of the) temperature of this system. All the variables and equations that we deal with are adimensional. As the system is multidimensional, we present the results in temporal graphs (variables vs time) and phase-space graphs (two physical variables plot against each other).

In all cases, we take the same mathematical form for the friction law, $G(v) = (|v| + 10^{-4})$, as used in the previous works (see, for instance, [2,7,8]), for a similar model of thermosyphon with a non-viscoelastic fluid with one component. The rationale behind this equation is that it interpolates between a constant (low Reynolds number laminar flow) and a linear (highly turbulent flow) function of the velocity. Likewise, A and B , which refer to the position-dependant (x) heat flux inside the loop will be used as tuning parameters. We will assume $A = 0$ in order to simplify, as different values of A only changes the *phase* the periodic function $h(x)$. We will also fix $B = 50$ the heat flux parameter, $\nu = 0.002$ the diffusion coefficient and observe the evolution of the variables. The initial conditions are fixed to $w(0) = 0, v(0) = 0, a^1(0) = 1, a^2(0) = 1$. Finally, we have also studied the behavior of the system of equations by keeping ε as a tuning parameter ranging from 1 to 10, to observe the response of the system under the effects of viscoelasticity.

3.2 The chaotic behavior of the model

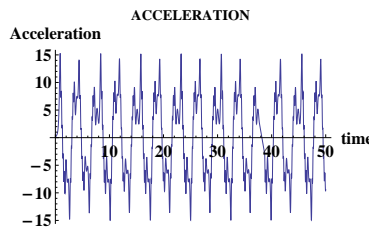


Fig. 1. The time evolution of the acceleration, $w(t)$, with $\varepsilon = 1, A = 0, B = 50, \nu = 0.002$ and $G(v) = (|v| + 10^{-4})$

The impact of ε on the system has been keenly observed for various parameters. In general (see below), as the viscoelastic component ε increases, the chaotic behavior of the system also increases. In Fig. 1 we show the time evolution of the acceleration, $w(t)$, for the viscoelastic parameter $\varepsilon = 1$. The acceleration $w(t)$ ranges from -15 to 15. The plot is chaotic but, although this is more apparent in the acceleration plot than in the velocity one. This is reasonable as the velocity is the time integral of the acceleration, namely, the velocity curve looks smoother than that of acceleration (therefore the chaotic behavior is not so apparent).

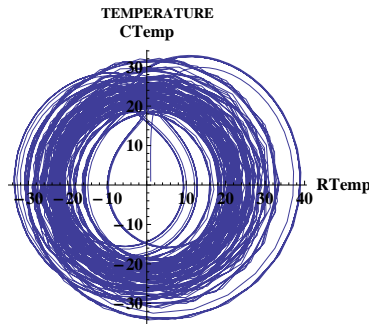


Fig. 2. Phase-plane of the real and imaginary parts of Fourier transform of the temperature for $\varepsilon = 1$, $A = 0$, $B = 50$, $\nu = 0.002$ and $G(v) = (|v| + 10^{-4})$.

In Fig. 2 we show the phase-diagram for the real $a^1(t)$ and imaginary $a^2(t)$ parts of the Fourier transform of the temperature. As expected, the trajectory in this phase-plane moves inwards and outwards. This plot illustrates the underlying complex dynamics of the attractor as a two dimensional projection.

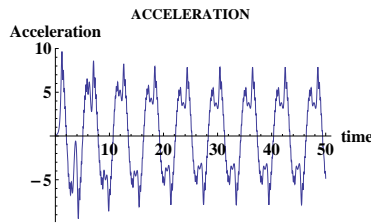


Fig. 3. The time evolution of the acceleration, $w(t)$, with $\varepsilon = 3$, $A = 0$, $B = 50$, $\nu = 0.002$ and $G(v) = (|v| + 10^{-4})$

In the second set of numerical experiments we increase the value of viscoelastic component to $\varepsilon = 3$. As the value of viscoelastic component ε is relatively higher than the previous experiment i.e., ($\varepsilon = 3$) the system tends to be more chaotic than the previous experiment. The acceleration $w(t)$ ranges from -10 to 10. The deviation in the progress of acceleration is maintained till the end of the progress. Apparently, the behavior is also chaotic but this chaos seems to be embedded in larger timescale oscillations. Interestingly, the number of oscillations is reduced from 15 to 9, Fig. 3 showing less number of peaks than the first case. This is a reflection of the memory effects associated to the viscoelastic of the fluid. Thus, as ε plays the role of a time scale, the larger this value the longer are the memory effects (in our case exposed through the period of the underlying oscillations).

For $\varepsilon = 10$ (Fig. 4), the system still exhibits a chaotic progression, with the acceleration ranging from -4 to 4 and with even an underlying longer-period oscillations compared to the previous experiments.

Finally, in Fig. 5 we show the phase-diagram for $a^1(t)$ and $a^2(t)$. Again, as expected, the trajectory in this phase-plane moves inwards and outwards.

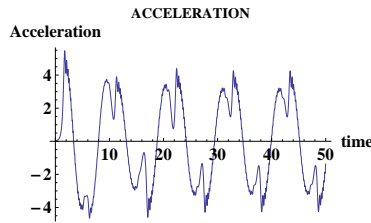


Fig. 4. The time evolution of the acceleration, $w(t)$, with $\varepsilon = 10$, $A = 0$, $B = 50$, $\nu = 0.002$ and $G(v) = (|v| + 10^{-4})$

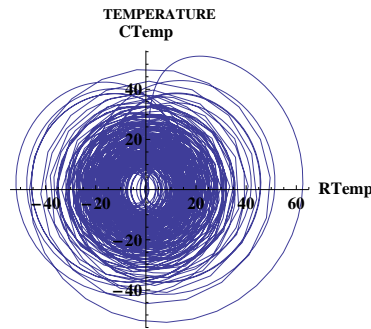


Fig. 5. Phase-plane of the real and imaginary parts of Fourier transform of the temperature for $\varepsilon = 10$, $A = 0$, $B = 50$, $\nu = 0.002$ and $G(v) = (|v| + 10^{-4})$.

This plot illustrates the underlying complex dynamics of the attractor of a two dimensional projection.

In summary, larger values of the viscoelastic parameters ε , results in sustained chaotic behaviors overlapped with an (almost) periodic behavior whose period scales with the numerical value of ε . The dynamics becomes more complex and is characterized in all cases by periods of chaos and of violent oscillations, giving an idea of the complexity of the solutions of the system under these variables due to memory effects.

4 Conclusion

The physical and mathematical implications of the resulting system of ODEs which describe the dynamics at the inertial manifold is analyzed numerically. The role of the parameter ε which contains the viscoelastic information of the fluid was treated with special attention. We studied the asymptotic behavior of the system for different values of ε the coefficient of viscoelasticity. We can conclude that for larger values of ε the system behaves more chaotic. Physically, this induction of chaotic behaviors is related to the memory effects inherent to viscoelastic fluids. Thus, in the same way as delayed equations are known to produce chaos, even in the simplest situations, viscoelasticity produces the same kind of transition.

Acknowledgements

This work has been partially supported by Projects MTM2009-07540, GR58/08 Grupo 920894 BSCH-UCM, Grupo de Investigación CADEDIF and FIS2009-12964-C05-03, SPAIN.

References

- 1.A. Jiménez-Casas, Mario Castro, and Justine Yasappan. Finite-dimensional behavior in a thermosyphon with a viscoelastic fluid. submitted, 2012.
- 2.Justine Yasappan, A. Jiménez-Casas, and Mario Castro. Asymptotic behavior of a viscoelastic fluid in a closed loop thermosyphon: physical derivation, asymptotic analysis and numerical experiments. submitted, 2011.
- 3.J.B. Keller. Periodic oscillations in a model of thermal convection. *J. Fluid Mech.*, 26:599–606, 1966.
- 4.P. Welander. On the oscillatory instability of a differentially heated fluid loop. *J. Fluid Mech.*, 29:17–30, 1967.
- 5.J.J.L. Velázquez. On the dynamics of a closed thermosyphon. *SIAM J. Appl. Math.*, 54:1561–1593, 1994.
- 6.F. Morrison. Understanding rheology. *Oxford University Press, USA*, 2001.
- 7.A. Jiménez-Casas, and A.M-L. Ovejero. Numerical analysis of a closed-loop thermosyphon including the Soret effect. *Appl. Math. Comput.*, 124:289-318, 2001.
- 8.A. Rodríguez-Bernal, and E.S. Van Vleck. Diffusion Induced Chaos in a Closed Loop Thermosyphon. *SIAM J. Appl. Math.*, 58:1072-1093, 1998.